

On the Trade-off Between AoI Performance and Resource Reuse Efficiency in 5G NR V2X Sidelink

Alexey Rolich*, Mert Yildiz*, Ion Turcanu[†], Alexey Vinel[‡], and Andrea Baiocchi*

*Dept. of Information Engineering, Electronics and Telecommunications (DIET), University of Rome Sapienza, Italy

[†]Luxembourg Institute of Science and Technology (LIST), Luxembourg

[‡]Karlsruhe Institute of Technology (KIT), Karlsruhe, Germany

alexey.rolich@uniroma1.it mert.yildiz@uniroma1.it ion.turcanu@list.lu
alexey.vinel@kit.edu andrea.baiocchi@uniroma1.it

Abstract—In 5G New Radio (NR)-Vehicle-to-Everything (V2X) Mode 2 sidelink, vehicles autonomously select resources for periodic broadcasts using either Dynamic Scheduling (DS) or Semi-Persistent Scheduling (SPS). SPS typically reduces collisions by selecting radio resources based on channel sensing and persisting on the same radio resource, which is shown to improve efficiency of spatial reuse. However, our study shows that this does not always improve the Age of Information (AoI). Persistence induces bursts of message losses, creating extended gaps between successful updates. Consequently, DS – despite potentially achieving lower Packet Delivery Ratio (PDR) – often achieves better AoI for realistic performance targets. These findings reveal a fundamental trade-off between reliability (PDR) and timeliness (AoI) and highlight the need for careful persistence management in vehicular communication systems.

I. INTRODUCTION

Intelligent Transportation Systems (ITS) rely on continuous exchange of update messages among vehicles, pedestrians, and infrastructure to enable cooperative awareness and collective perception. These capabilities are critical for a multitude of advanced safety features and autonomous driving functions. In this context, 5G New Radio (NR)-Vehicle-to-Everything (V2X) emerges as a key enabling technology, supporting sidelink communications through its Mode 2 operation.

Mode 2 allows vehicles to autonomously select and reserve resources to transmit periodic messages, such as Cooperative Awareness Messages (CAMs) or Basic Safety Messages (BSMs), by means of either Dynamic Scheduling (DS) or Semi-Persistent Scheduling (SPS) algorithms [1], [2]. In particular, while DS has been designed for aperiodic, event-driven messages, SPS is often seen as more efficient for periodic broadcast messaging – needed for cooperative awareness – because it reserves radio resources over multiple consecutive transmissions, mitigating collisions and improving the reliability of communications. Several studies [3]–[7] confirm that SPS outperforms DS in terms of throughput, Packet Delivery Ratio (PDR), and Packet Inter-Reception Delay (PIR) for periodic traffic flows, especially as the persistence degree of resource usage increases.

In this paper, we highlight the underlying process that originates such improvements and show that persistence brings more order to the spatial and temporal reuse of sidelink resources, namely Sub-Channels (SCs). Despite being a random

multiple access algorithm and dealing with nodes whose (relative) positions can be modeled as random, SPS still induces even spacing between successive vehicles using the same SC, thanks to the sensing function and the slowing of SC reselection induced by persistence. This finding highlights the critical role of persistence management in scenarios requiring structured resource reallocation, such as vehicle platooning [8] or train communication systems [9], and underscores its contribution to improving communication stability.

Despite these known benefits, a key gap in the existing literature is understanding how resource scheduling strategies (DS vs. SPS) impact *time-critical* performance metrics such as the Age of Information (AoI). While higher PDR indicates reliable communication, the *timeliness* of delivered messages is equally crucial: lost messages arriving in consecutive “bursts” can lead to prolonged information blackouts, severely degrading the freshness of updates in real-world driving scenarios. Although SPS achieves more order in the spatial and temporal reuse of sidelink resources, its inherent persistence can amplify bursty message losses under certain network conditions, raising questions about its suitability for scenarios where AoI requirements matter. By contrast, DS – though simpler and less efficient in terms of PDR – may occasionally offer better AoI performance due to more randomized resource selections.

To address this gap, this paper provides an in-depth study of how persistence in resource allocation affects the interplay between reliability (PDR) and timeliness (probability of AoI exceeding a given threshold) in 5G NR-V2X sidelink communications. Our contributions can be summarized as follows:

- We demonstrate that while SPS’s structured resource reuse improves PDR, it can simultaneously degrade AoI due to bursty message losses, especially at higher persistence levels.
- We show that DS – being simpler and non-persistent – outperforms SPS in terms of AoI, even under periodic messaging traffic patterns, especially for looser AoI constraints.
- We highlight how managing persistence is critical for scenarios requiring structured resource reuse, indicating a need for careful algorithmic parameter selection to balance reliability and timeliness.

The rest of the paper is organized as follows. In Section II, we review related works focusing on the investigation of persistence and reuse distance in 5G NR-V2X sidelink communication. Section III state the system model and details the simulation environment. In Section IV, we define key evaluation metrics, analyze the simulation results and discuss how resource allocation strategies affect PDR and AoI performance metrics. Finally, Section V concludes the paper.

II. BACKGROUND AND RELATED WORKS

Reuse distance plays a key role in optimizing 5G NR-V2X networks by enabling efficient resource reuse while minimizing interference. A Reuse Distance-Aided Resource Selection (RD-RS) mechanism has been proposed in [10] to integrate reuse distance constraints into SPS, leading to a 9% improvement in Packet Reception Ratio (PRR) and a 70% reduction in inter-packet gaps. In Full-Duplex (FD) NR-V2X, effective self-interference cancellation shortens reuse distances compared to Half-Duplex (HD) systems [11].

To enhance reuse distance, frequency reuse strategies have been widely explored. One approach divides resources into inner and outer zones to mitigate interference in C-V2X Mode 3, utilizing Full Frequency Reuse (FFR) and Partial Frequency Reuse (PFR) schemes [12]. Extending this concept, Fu et al. [13] propose a Per-Zone Resource Reuse (PZRR) technique that partitions road areas, allowing non-adjacent zones to reuse resources, improving message delivery rates and Vulnerable Road User Protection (VRUP).

Adaptive reuse distance mechanisms have proven effective in dense vehicular networks. In [14], a stochastic geometry-based model dynamically adjusts reuse distance through paired sensing and adaptive power control, achieving a 27% PRR increase and 95% system reliability under high traffic conditions. Another study [15] examines the impact of big vehicle shadowing in LTE and 5G V2X, showing that relay-assisted communication enhances coverage and reuse efficiency.

In [16] aperiodic traffic management in NR-V2X has been improved by the Reservation for Aperiodic Packets (RAP) method, which enhances PRR and extends Tx-Rx distances by 75 m compared to standard SPS. Machine learning has also been applied to optimize persistence probability in aperiodic CAM transmission, dynamically adjusting resource reservations based on predicted traffic patterns by [17].

A comparative study [4] of SPS and DS finds that SPS performs better for periodic traffic, while DS is more effective for aperiodic transmissions. An adaptive scheduling strategy dynamically switches between the two, optimizing performance in mixed traffic scenarios. Resource allocation for platooning under hidden node conditions has also been explored [18], integrating an Improved Random Selection scheme with a Deep Deterministic Policy Gradient algorithm, though persistence in SPS remains underexplored.

Security vulnerabilities in SPS arise from predictable resource reservations, making it susceptible to attacks [19]. To counter this, a defense mechanism incorporating fuzzy logic and

feedback-based attack detection dynamically adjusts Reselection Counter (RC), improving system security through enhanced persistence management. Chourasia et al. [20] propose a traffic-aware variant of SPS (TA-SPS) that dynamically adjusts RC and persistence probability, leading to a 4% PRR improvement in time-varying traffic scenarios.

In our previous works [6], [7] we analyzed the role of persistence in SPS, particularly its impact on AoI, through analytical modeling and ns-3 simulations. These studies identified optimal persistence parameters to minimize AoI under controlled communication conditions, and were later extended to account for distance-dependent propagation, enriching our understanding of how persistence influences sidelink performance.

In contrast, the present paper introduces a substantial advancement by exploring a more realistic communication setting characterized by hidden nodes – an aspect previously overlooked. Specifically, it investigates the interplay between persistence and the order of resource reuse, a key factor in environments where spatial reuse is critical. While persistence and reuse distance have been individually studied in terms of AoI, PRR, collisions, and interference, their combined effect has not yet been addressed.

III. SYSTEM MODEL

We consider a highway scenario, with multiple lanes and two opposite directions. More in depth, the scenario involves a 5000 m stretch of highway with three lanes in each direction. Vehicles travel at 70 km/h, resulting in a minimum safe headway distance of 40 m with typical reaction time and breaking deceleration. Hence, the highest possible vehicle density is 150 veh/km. In the following we assume a high traffic volume, with average density of 140 veh/km.

Vehicle mobility, propagation channel, physical channel and multiple access functionality are simulated by using the ns-3 based MoReV2X simulation tool [21]. This module focuses on sub-6 GHz NR-V2X communications, implementing NR V2X Mode 2 sidelink, with direct vehicle-to-vehicle data exchange via distributed access, either with DS and SPS mechanisms. Additionally, Wireless Blind Spot (WBS), as described in [22], is accounted for in the ns-3 MoReV2X simulator.

Throughout the simulations, the Orthogonal Frequency-Division Multiple Access (OFDM) numerology is set to 0, resulting in an Sub-Carrier Spacing (SCS) of 15 kHz and a slot duration of $t_s = 1$ ms. NR-V2X radios are configured to operate on a 10 MHz channel within the 5.9 GHz ITS band, using SCs of 50 Resource Blocks (RBs). Consequently, there is one SC available per time slot. Modulation and Coding Scheme (MCS) 13 is selected, corresponding to 16-QAM with code rate 490/1024. The transmit power is set to 23 dBm, and the Received Signal Strength Indicator (RSSI) threshold to -92.3 dBm, which is 3 dB higher than the thermal noise floor, including a 9 dB noise figure.

Path loss and shadowing follow the models described in [23]. To account for fast-fading impairments affecting the Transport Block (TB) and Sidelink Control Information (SCI)

Table I
NUMERICAL VALUES OF MAIN SYSTEM PARAMETERS.

Parameter	Values
Highway length, L	5000 m
Vehicle density, ρ	140 veh/km
Number of lanes	6
Vehicle speed	70 km/h
RRI	100 ms
Message generation time, T_{gen}	100 ms
Channel bandwidth, BW	10 MHz
OFDM numerology, μ	0
Sub-Carrier Spacing, B_{sc}	15 kHz
Time slot duration, T_s	1 ms
MCS	MCS-13
Modulation	16 QAM
Code rate	0.4875 (490/1024)
# of RBs per Sub-Channel	50
# of Sub-Channels per time slot, n_{sc}	1
Transmission power	23 dBm
RSSI threshold (used for sensing)	-92.3 dBm
Noise power	-95.3 dBm
Log-normal shadowing standard deviation, σ_{sh}	3 dB

Physical Layer performance, MoReV2X incorporates Block-Error Rate (BLER) curves from [24]. These curves exhibit a quite sharp transition around 5–6 dB. Assessment of outcome of transmissions is therefore evaluated as follows. The Signal-to-Noise-plus-Interference Ratio (SNIR) at a receiver node j for the transmission of a message by node i is evaluated as

$$\text{SNIR} = \frac{G_{r_{ij}} G_{\text{sh},ij} P_{\text{tx}}}{P_N + P_{\text{tx}} \sum_{k \in \mathcal{I}_{ij}} G_{r_{kj}} G_{\text{sh},kj}} \quad (1)$$

where r_{ij} is the distance between nodes i and j , $G(\cdot)$ is the distance dependent path gain, $G_{\text{sh},ij}$ is the log-normal shadowing gain (with standard deviation $\sigma_{sh} = 3$ dB), and \mathcal{I}_{ij} is the set of nodes that interfere with the reception of the message from i at the receiving node j , i.e., those nodes that transmit using the same SC as node i does. The value obtained for SNIR_{ij} is used as an input to the look-up table that implements the BLER curve in the simulation code. The corresponding BLER probability is used to decide whether the considered reception at node j is decoded successfully.

At the Medium Access Control (MAC) sub-layer, the Resource Reservation Interval (RRI) is the same for all nodes, set to 100 ms. As a result, the number of available SCs in one RRI period equals $K = 100$ (one SC per slot, with slot time equal to 1 ms in the baseline numerology). Moreover, T_0 is set to a number of slots equivalent to 1100 ms, the initial Reference Signal Receive Power (RSRP) threshold is set to -120.27 dBm, and β is set to 20%. For optimal SPS performance, periodic traffic is employed, with a message generation interval of $T_{\text{gen}} = 100$ ms.

In SPS, persistence is realized by means of the RC and persistence probability P . The former defines the initial value of the countdown counter that rules the number of consecutive uses of a same selected SC. It is chosen uniformly at random in the interval $[5, 15]$ in case RRI is no less than 100 ms. The persistence probability P is set to a value in the interval $[0, 0.8]$. When the RC hits 0, with probability P the node retains the

same SC and draws a new value of its RC. With probability $1 - P$, a new SC is selected uniformly at random among those sensed as idle in the selection window.

We introduce an additional parameter, already defined in [6], [7], for later use in the performance evaluation: the *jump probability*

$$q = \frac{1 - P}{\overline{RC}} \quad (2)$$

where \overline{RC} is the mean value of RC (equal to 10 in case $\text{RRI} \geq 100$ ms.) The parameter q gives the probability that a node leaves its currently used SC, assuming a Geometric probability distribution of the number of consecutive uses of the selected SC. In our analysis, we utilize q as the primary parameter for the resource allocation mechanism, enabling a comprehensive investigation of the impact of persistence on the spatial and temporal reuse of radio resources, even beyond the range constraints imposed by the standard.

Numerical values of main parameters are listed in Table I.

IV. PERFORMANCE EVALUATION

In this section, we introduce the adopted performance metrics (Section IV-A), we discuss the value of ordered reuse of resources (Section IV-B), and we analyze the SC reuse over space (Section IV-C) and time (Section IV-D). Finally, we address performance analysis in terms of AoI (Section IV-E).

A. Metrics

To investigate the interplay between communication reliability and timeliness, we consider two key metrics: (i) the Coefficient of Variation (COV) of the spatial and temporal order of resource reuse, which correlates with reliability, and (ii) the AoI, which reflects timeliness.

Since all nodes use the same RRI, we can divide the time axis into frames consisting of K consecutive SCs. For a given SC, let $x_j(t)$, $j = 1, \dots, n_t$ denote the position of the j -th node using that SC in frame t , and assume that $x_1(t) \leq x_2(t) \leq \dots \leq x_{n_t}(t)$. The reuse distance can be evaluated as $D_j(t) = x_{j+1}(t) - x_j(t)$, $j = 1, \dots, n_t - 1$. The corresponding average reuse distance, obtained by averaging over j and over T frames is given by

$$\overline{D} = \frac{\sum_{t=1}^T \sum_{j=1}^{n_t-1} D_j(t)}{\sum_{t=1}^T (n_t - 1)} \quad (3)$$

The average square values of the reuse distance can be evaluated analogously:

$$\overline{D}_2 = \frac{\sum_{t=1}^T \sum_{j=1}^{n_t-1} D_j(t)^2}{\sum_{t=1}^T (n_t - 1)} \quad (4)$$

Then, a measure of spatial reuse disorder is given by the COV of the reuse distance:

$$\text{COV}_D = \frac{\overline{D}_2 - (\overline{D})^2}{(\overline{D})^2} \quad (5)$$

An entirely similar analysis can be carried out on the samples $Q_k(t)$ defined as the number of nodes simultaneously utilizing

SC k in frame t , $k = 1, \dots, K$, for $t = 1, \dots, T$. As a result, the COV of the number of nodes using a given resource is evaluated, denoted with COV_Q . This is a metric of temporal order of SC usage, while COV_D gives a measure of spatial order or SC usage.

As for AoI, let $Y_{ij}^{(k)}$ be the time gap between the $(k-1)$ -th and the k -th successfully received messages from i to j , for $k \geq 2$. For a given couple of nodes (i, j) , where i originates updates messages and j receives them, the probability of AoI violating a given threshold A_{th} is estimated as follows.

$$V_{ij}(A_{\text{th}}) = \frac{\sum_{k=2}^{m_{ij}} \max\{0, Y_{ij}^{(k)} - A_{\text{th}}\}}{\sum_{k=2}^{m_{ij}} Y_{ij}^{(k)}} \quad (6)$$

where m_{ij} is the number of collected AoI samples for a given couple of nodes (i, j) .

This metric is evaluated only for those couples for which $m_{ij} \geq m_0$, where we set $m_0 = 5$. Let \mathcal{N} denote the set of all ordered couples (i, j) of nodes such that $m_{ij} \geq m_0$ and let $|\mathcal{N}|$ denote its cardinality. A global probability of AoI violation metric V is obtained from individual values of V_{ij} , by averaging over the set \mathcal{N} .

Both V_{ij} and V can be evaluated by restring the analysis to couples within distance r , i.e., with a distance between nodes i and j in the interval $(0, r]$. In this case, we use the notation $\bar{A}_{ij}(r)$ and $V(r, A_{\text{th}})$ respectively.

B. Value of ordered spatial reuse

We show that the improvement in PDR performance provided by SPS over DS under periodic message traffic flows results from better-ordered spatial reuse of SCs. Specifically, sensing reduces the probability that nearby nodes select the same SC, thereby lowering the risk of excessive interference.

To appreciate how valuable ordered spatial reuse of resources is, we compare two situation in a simplified scenario. We consider equally spaced out vehicles along a road, i.e., the headway distance between consecutive vehicles is equal to $1/\delta$, where δ is vehicle density. The most ordered (and efficient) reuse of the available K SCs can be achieved by means of an ideal centralized scheduling that assigns SC j to vehicles in positions $(j + mK)/\delta$, $m \in \mathbb{Z}$, i.e., the same SC is orderly assigned to each one vehicle out of K consecutive ones (round-robin scheduling over K resources). Then, the reuse distance is $D = K/\delta$ and SNIR at distance x between transmitter and receiver can be expressed as follows:

$$\text{SNIR}(x) = \frac{G(x)G_{\text{sh}}P_{\text{tx}}}{P_{\text{N}} + P_{\text{tx}} \sum_{k=1}^{\infty} (G(kD-x)G_{\text{sh},k} + G(kD+x)G'_{\text{sh},k})} \quad (7)$$

where G_{sh} , $G_{\text{sh},k}$ and $G'_{\text{sh},k}$ denote independent log-normal shadowing gains. The PDR can be evaluated as the probability that SNIR(x) exceeds the threshold for the considered MCS. Figure 1 shows the plot of PDR with the described centralized reuse of SCs as a function of distance (blue curve). It is compared with the PDR in case of purely random SC assignment, where each vehicle draws uniformly at random

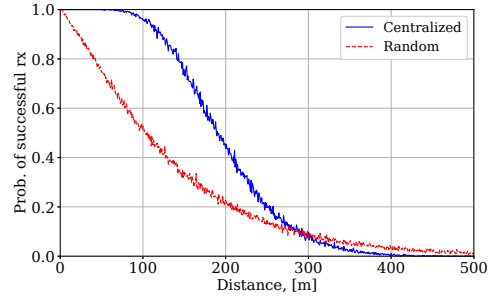


Figure 1. PDR as a function of distance for centralized (blue) and random (red) scheduling of SCs on a sequence of evenly spaced out vehicles with density of 140 veh/km (see Section III for details).

which SC is used, independently of any other vehicle (red curve). This models what DS achieves.

The advantage of centralized scheduling, which maximizes the affordable reuse distance, given the available resources, is that it extends as far as possible the range of sender-to-receiver distances within which reception is almost surely successful. Then, PDR performance falls to zero quite sharply, with a narrow transition region. This behavior is close to the ideal on-off limit, where reception is always successful, provided distance is below a suitable threshold. On the contrary, with random SC assignment, hence a most disordered reuse, PDR is significantly less than one even for very small values of the distance, and it drops steadily as the distance grows, resulting in severely less reliable communications.

By providing some order in SC reuse, SPS strives to achieve what a centralized planning could provide. While this is beneficial for PDR, hence for PIR and throughput, we will show that it turns out to be controversial when the target performance metrics is related to AoI.

C. Analysis of SC spatial reuse

Thanks to sensing in SPS, nodes measure signal levels in the SCs and compile a list of idle SCs based on the previous frame. These idle SCs, which serve as candidates for future reservation, are identified by each node using the RSSI, which primarily reflects the distance between the sensing node and the transmitters using the considered SC.

Consequently, it is possible to define a distance between vehicles, D_{reuse} , that allows for the safe reuse of the same SC with minimal interference, reducing the risk of collisions. Reuse distance is evaluated by considering the distance between consecutive vehicles using the same SC in a given RRI according to Equation (3).

In an ideal scenario, when operating in 5G NR-V2X Mode 1, the base station acts as an optimal scheduler with full knowledge of the distances between nodes, ensuring efficient resource allocation, including optimal resource reuse. In this ideal case, nodes reusing the same SC would be spaced out by a fixed distance (disregarding the randomness due to

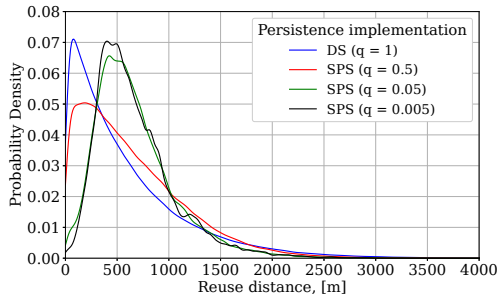


Figure 2. Empirical PDF of reuse distance for persistence levels and vehicle density equal to 140 veh/km. The q values used are as follows: DS is represented by $q = 1$, weak persistence by $q = 0.5$, moderate persistence (according to standard SPS) by $q = 0.05$, and strong persistence by $q = 0.005$.

specific vehicle position along the road). With such an ideal deterministic reuse, we get:

$$D_{\text{reuse}}^* = \frac{K}{\rho} \quad (8)$$

where ρ is the vehicle density and K is the number of SCs/RRI.

In our scenario, the numerical value of D_{reuse}^* for resource reuse is 713 m. However, in real-world conditions, this value represents only the *mean* value of the reuse distance. Sources of randomness in the reuse distance values are random positions of vehicles along the road and the distributed algorithms for the selection of SCs in 5G NR-V2X Mode 2 sidelink. This randomized SC spatial reuse results in lower reuse efficiency, in case the reuse distance between two consecutive vehicles is larger than D_{reuse}^* . If, on the contrary, the reuse distance is smaller than D_{reuse}^* , it increases the likelihood of collisions.

Empirical PDFs of reuse distance are shown in Figure 2 for different levels of persistence. Four lines are depicted, each corresponding to a specific persistence level. In the case of an ideal scheduler, D_{reuse} would be a deterministic quantity. The spread of the PDFs gives an indication as to the disorder in reuse due to the self-organized resource selection in 5G NR-V2X Mode 2 (an instance “price of anarchy”). The PDF is shifted to lower values in case of DS, which is consistent with the absence of sensing¹, hence the possibility of reusing the same channel even for nearby nodes. As persistence increases, a distinct peak begins to emerge, becoming more pronounced with higher persistence levels, and shifting towards the 400–500 m range. This indicates that persistence helps reduce the number of collisions by encouraging spatial separation between nodes using the same SC.

Figure 3 illustrates how spatial reuse of resources varies across different persistence levels. It shows the COV_D , calculated according to Equation (5), as a function of q . Red markers show the performance of the standard SPS. The blue line illustrates the implementation of persistence with Geometric

¹Sensing is useless with DS, if *all* SCs are handled by DS. In a mixed situation, where nodes using SPS share the sidelink resources with nodes using DS, all nodes must implement sensing, including those using DS. In that case, a node using DS selects an SC at random among those that are not reserved by SPS nodes, as reported in the SCL.

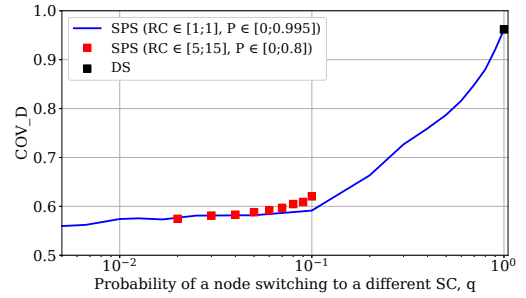


Figure 3. Coefficient of variation of SC reuse distance as a function of q

probability distribution of RC, based on q . DS is represented by a single black marker.

Most notably, a clear trend emerges: COV_D decreases monotonically with even slight increases in persistence, reinforcing our hypothesis that higher persistence levels introduce greater order and regularity in the spatial reuse of SCs. This helps limiting the effect of interference and ultimately collisions.

We also observe that the performance values of the standard SPS closely align with those of the Geometric probability distribution of RC within the moderate persistence zone. Also, the COV_D value close to 1 for DS matches the fact that the reuse distance with DS has an approximately Geometric probability distribution. If d_j denotes the distance between two consecutive vehicles (the j -th and $(j+1)$ -th along the road), the reuse distance with DS is $D = \sum_{j=1}^N d_j$, where N is distributed according to a Geometric probability distribution of RC mass function: $\mathcal{P}(N = h) = (1 - 1/K)^{h-1} \cdot 1/K$, $h \geq 1$. Since the distances d_j exhibit a relatively low variability at the considered vehicle density of 140 veh/km, with an average speed of 70 km/h, we can approximate d_j with a constant d , hence D turns out to be Geometrically distributed.

The spatial order of SC reuse is particularly critical for applications that are sensitive to variations in D_{reuse} values, such as the use of 5G NR-V2X sidelink communication to connect railway carriages in a multi-hop network [9], [25]. Regardless of the application, improving the spatial order of radio resource reuse (i.e., reducing the COV_D) leads to more efficient resource utilization. On the one hand, it minimizes collisions by preventing neighboring vehicles from selecting the same SC. On the other hand, it reduces gaps in resource allocation, thereby reducing idle resources and inefficiencies.

It is equally important to align resource allocation strategies with the performance requirements specific to each application. Our analysis in [6], [7] shows that while strong persistence improves the spatial ordering of resource reuse, it significantly increases AoI. Therefore, applications must establish customized constraints for these metrics to identify the optimal persistence class configuration that best suits their use case.

D. Analysis of SC reuse over time

In this section, we analyze the impact of persistence on resource usage dynamics over time. Figure 4 illustrates the time evolution of the number of nodes using a tagged SC over

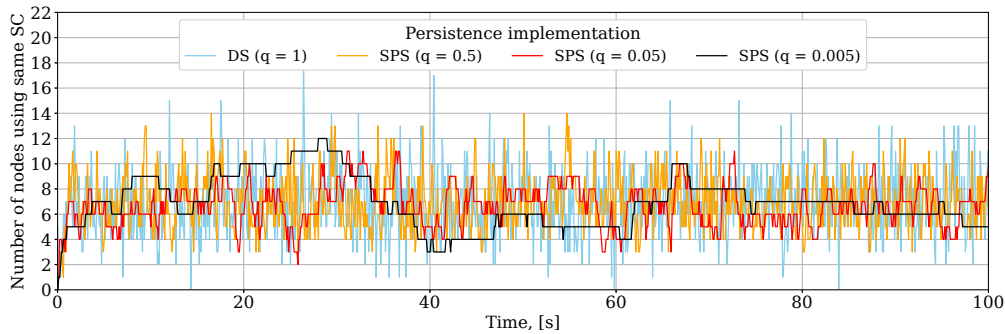


Figure 4. Number of the nodes using the a tagged SC over a time span of 100 s.

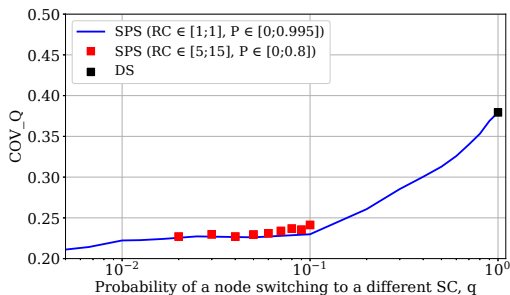


Figure 5. Coefficient of variation of the nodes number using the same SC at the same time frame as function of q .

a time span of 100 s^2 . The lines represent different persistence classes: blue for DS, orange for weak persistence, red for moderate persistence, and black for strong persistence.

As evident from Figure 4, higher persistence reduces fluctuations in the number of nodes concurrently using a SC (a trend observed for all SCs, as they are statistically equivalent). However, increased persistence slows switching when the RC reaches zero, effectively “freezing” the system. Interestingly, if we extend the time horizon to 10 000 s, the fluctuations in the number of nodes using strong persistence would resemble those of weak persistence over a shorter 100 s window. Despite this, for real-world applications, 100 s of vehicle movement is relevant to most automotive application, making this shorter time frame our primary focus.

To quantify how persistence influences the temporal ordering of SC usage by nodes, we analyze the COV_Q of the stochastic process $Q(t)$, i.e., the number of nodes using a tagged SC during the time period corresponding to the t -th RRI. Figure 5 displays COV_Q as a function of q , across all persistence levels, with color-coding consistent with other similar plots in Section IV-C.

For any level of persistence, the mean density of nodes using the tagged SC simultaneously remains constant at ρ/K , where ρ is the mean vehicle density on the road. Only the standard deviation of $Q(t)$ changes as we modify the persistence level.

²We refer to one given SC out of the K SCs belonging to an RRI period, since, in the considered setting, all SCs are statistically equivalent.

The results in Figure 5 clearly demonstrate that increasing persistence enhances the order of SC temporal usage, leading to greater usage uniformity across different SCs in terms of the number of nodes concurrently using each SC.

This higher uniformity of usage level induced by persistence reduces collisions. However, it is important to remember that temporal “freezing” of the system results in long-lasting collision events. This leads to poorer AoI performance as persistence is increased. Since collisions cannot be completely avoided, their prolonged duration may render the system unsatisfactory from a safety perspective. This effect will be further analyzed in Section IV-E.

E. AoI performance analysis

In this section, we analyze the impact of persistence in SPS and the use of DS on AoI performance. As the primary metric, we consider the probability of AoI violation, $V(r, A_{\text{th}})$, as defined in Section IV-A, Equation (6).

Figure 6 illustrates $V(r, A_{\text{th}})$ as a function of the communication range r . For each case, we fix the AoI threshold and evaluate the probability of exceeding it for DS (no persistence) and for standardized SPS persistence values of 0 and 0.8. Figure 6 consists of three subfigures: (a) $A_{\text{th}} = 0.1$ s, (b) $A_{\text{th}} = 0.2$ s, and (c) $A_{\text{th}} = 1$ s.

From this analysis, we observe that, while SPS benefits PDR through structured resource reuse, it can degrade AoI performance compared to DS as r and A_{th} increase. The probability of vehicle pairs exceeding the AoI threshold indicates that SPS improves AoI only under strict constraints (Figure 6a, $A_{\text{th}} = 0.1$ s). However, for more relaxed AoI targets ($A_{\text{th}} = 0.2$ s and $A_{\text{th}} = 1$ s), DS performs comparably or even outperforms SPS, even in periodic traffic scenarios. This distinction is crucial from the perspective of application-specific performance requirements, as they can vary significantly across different use cases.

This surprising result arises from SPS-induced bursty losses, which lead to extended update blackouts. While SPS reduces the overall loss rate, its persistence causes consecutive failures, impacting AoI more severely than the random message drops observed with DS. Although structured scheduling improves resource efficiency, AoI does not always correlate with efficiency. Furthermore, in 5G NR-V2X sidelink communications, SPS

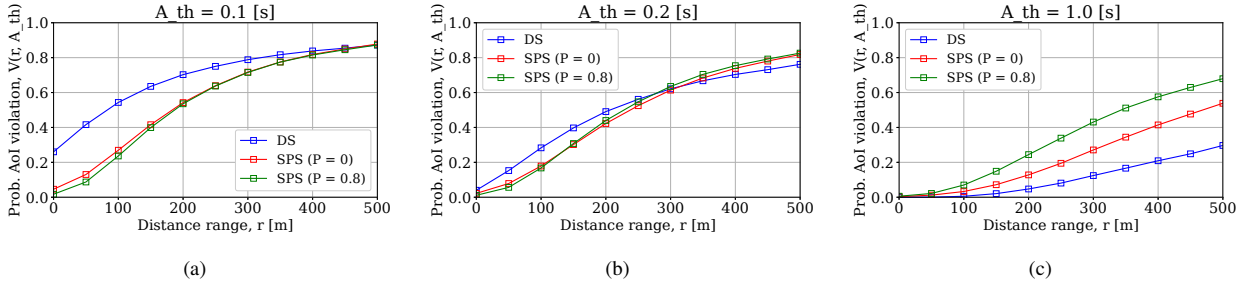


Figure 6. Probability of AoI violation as a function of distance range from ego-vehicle, r , with fixed of AoI threshold, A_{th} . This figure presents the performance of DS and the extreme values of P range for the standardized SPS.

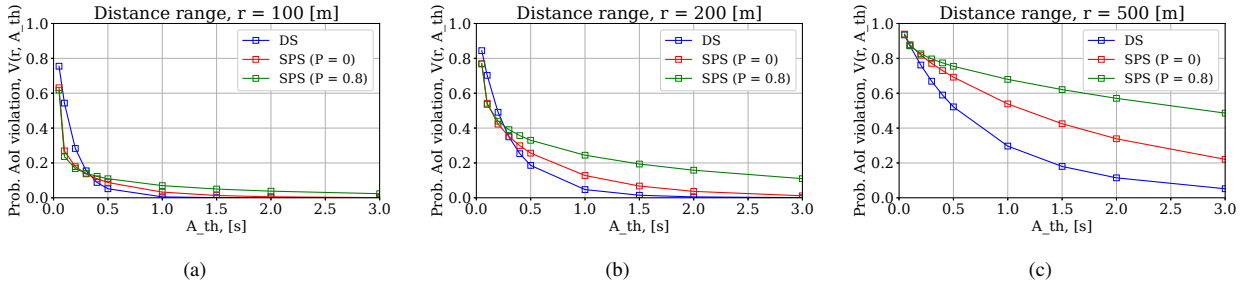


Figure 7. Probability of AoI violation as a function of AoI threshold, A_{th} , for fixed distance range from ego-vehicle, r . This figure presents the performance of DS and the extreme values of P range for the standardized SPS.

operates in a randomized distributed manner, unlike centralized scheduling (e.g., 5G NR-V2X Mode 1), which achieves superior PDR and AoI but remains impractical due to its high complexity and signaling overhead compared to DS.

A similar trend can be observed in Figure 7, which presents the inverse analysis. Here, we fix the communication radius r and examine the probability of exceeding the AoI threshold as a function of A_{th} . This analysis provides an application-specific perspective on achievable performance at a given distance from the node based on the chosen threshold. Figure 7 consists of three subfigures: (a) $r = 100$ m, (b) $r = 200$ m, and (c) $r = 500$ m. From this analysis, we observe that for a communication radius below 200 m, DS exhibits slightly lower but comparable performance to SPS up to $A_{th} = 0.3$ s. For larger values of A_{th} , DS demonstrates superior performance, and as r increases, the performance gap widens significantly.

Ultimately, when weighing the trade-off between high persistence, which supports structured resource reuse, and low persistence, which enhances the freshness of periodic messages, it is crucial to consider the specific application requirements of the scenario. These requirements may vary considerably. In ITS applications, reuse order is vital for coordinated tasks like platooning, virtual train coupling [9], and intersection management, while keeping AoI below a threshold is key for safety-critical cases such as collision avoidance, vulnerable road user protection, and autonomous driving in dense environments [26]. Therefore, selecting an appropriate resource allocation mechanism and configuring parameters like persistence is essential to optimize communication efficiency under given constraints and performance demands.

V. DISCUSSION AND CONCLUDING REMARKS

In this paper, we investigated the impact of persistence on the spatial and temporal order of radio resource reuse in vehicular highway scenarios, leveraging 5G NR-V2X sidelink communications. In spite of more ordered resource reuse, which is beneficial to performance metrics such as PDR and throughput, it turns out that SPS may provide worse performance with respect to DS in terms of AoI. Specifically, we have shown the following:

- In case hard limits are prescribed for AoI performance, persistence can bring some benefit in terms of AoI-related metric with respect to DS.
- Under more relaxed AoI performance targets, DS is definitely outperforming SPS even if the considered messaging traffic is periodic.

The reason for this seemingly counter-intuitive behavior is the increased burstiness of message losses due to persistence. While the average message loss rate is lower with SPS, the longer the persistence level, the more losses occur in a row. Such burstiness leads to update blackouts, which severely degrade AoI performance. In fact, timely message delivery does not require that *all* or *most* messages are safely delivered to the destination nodes, but rather that *updates are successfully delivered often enough*. In other words, as far as AoI is concerned, it is better to lose one message out of two purely at random than to lose occasionally ten messages in a row.

This conclusion is not in contradiction with long-established evidence that order generally brings superior efficiency in resource usage. Centralized scheduling actually achieved superior performance both in terms of PDR and AoI, since disruptive

collisions are ruled out by construction. The failure of SPS to achieve the same performance as centralized scheduling, even though it promotes ordered radio resource reuse, is a form of price of anarchy, stemming from its distributed character. However, centralized control is not preferable due to its exceedingly high complexity and signaling burden. Improvement of DS and SPS could be pursued by adaptive tuning of parameters, the use of directive antennas, multi-packet reception via successive interference cancellation, and coding schemes inspired by unsourced multiple access.

In future work, we will also evaluate whether these insights hold in more complex and irregular traffic settings—such as urban scenarios with intersections, traffic lights, and buildings that obstruct radio propagation—which may amplify the challenges of distributed scheduling and further highlight the trade-offs involved.

ACKNOWLEDGMENT

This work was partially funded by Sapienza University of Rome under the "Progetti per Avvio alla Ricerca - Tipo 2" program (2024) for the project "Enhancing Resource Allocation Mechanisms in 5G NR-V2X Sidelink Communications: Optimization and Performance Evaluation" (prot. AR2241906D14C736) and grant RP123188F68315A5 titled "Modeling and optimization of sidelink communications in C-V2X 5G NR." It also received partial support from the Italian Ministry of University and Research (PRIN, project code 20223Y85JN) for "LOREN - Low-delay congestion control for real-time applications over the Internet" (CUP: B53D23002200006) and from the Luxembourg National Research Fund (FNR) through the CANDI project (INTER/ANR/22/17192457). Co-funded by the European Union. Views and opinions expressed are however those of the authors only and do not necessarily reflect those of the European Union or European Climate, Infrastructure and Environment Executive Agency (CINEA). Neither the European Union nor the granting authority can be held responsible for them. Project grant no. 101069576.

REFERENCES

- [1] European Telecommunications Standards Institute, "LTE; 5G; Overall description of Radio Access Network (RAN) aspects for Vehicle-to-everything (V2X) based on LTE and NR (3GPP TR 37.985 version 17.1.1 Release 17)," ETSI, TR 137 985 V17.1.1, Apr. 2022.
- [2] European Telecommunications Standards Institute, "5G; NR; Radio Resource Control (RRC); Protocol specification (3GPP TS 38.331 version 17.3.0 Release 17)," ETSI, TS 138 331 V17.3.0, Jan. 2023.
- [3] C. Campolo, V. Todisco, A. Molinaro, A. Berthet, S. Bartoletti, and A. Bazzi, "Improving Resource Allocation for beyond 5G V2X Sidelink Connectivity," in *2021 55th Asilomar Conference on Signals, Systems, and Computers*, 2021, pp. 55–60.
- [4] L. Lusvarghi, A. Molina-Galan, B. Coll-Perales, J. Gozalvez, and M. L. Merani, "A Comparative Analysis of the Semi-Persistent and Dynamic Scheduling Schemes in NR-V2X Mode 2," *Vehicular Communications*, p. 100 628, 2023.
- [5] A. L. Chelli et al., "NR-V2X for Cooperative Adaptive Cruise Control," in *2024 IEEE 100th Vehicular Technology Conference (VTC2024-Fall)*, 2024, pp. 1–7.
- [6] A. Rolich, I. Turcanu, A. Vinel, and A. Baiocchi, "Impact of Persistence on the Age of Information in 5G NR-V2X Sidelink Communications," in *21st Mediterranean Communication and Computer Networking Conference (MedComNet)*, Ponza Island, Italy: IEEE, Jun. 2023, pp. 15–24.

- [7] A. Rolich, I. Turcanu, A. Vinel, and A. Baiocchi, "Understanding the impact of persistence and propagation on the Age of Information of broadcast traffic in 5G NR-V2X sidelink communications," *Computer Networks*, vol. 248, 2024.
- [8] S. Santini, A. Salvi, A. S. Valente, A. Pescapé, M. Segata, and R. L. Cigno, "A consensus-based approach for platooning with intervehicular communications and its validation in realistic scenarios," *IEEE Transactions on Vehicular Technology*, vol. 66, no. 3, pp. 1985–1999, 2016.
- [9] S. Nikooroo, J. Estrada-Jimenez, A. Machalek, J. Harri, T. Engel, and I. Turcanu, "Mitigating Collisions in Sidelink NR V2X: A Study on Cooperative Resource Allocation," in *22nd Mediterranean Communication and Computer Networking Conference (MedComNet 2024)*, Nice, France: IEEE, Jun. 2024.
- [10] J. Yin and S.-H. Hwang, "Reuse Distance-Aided Resource Selection Mechanisms for NR-V2X Sidelink Communication," *Sensors*, vol. 24, no. 1, 2024. [Online]. Available: <https://www.mdpi.com/1424-8220/24/1/253>.
- [11] R. Aslani and E. Saberina, "Performance analysis of full duplex and frequency reuse in NR-V2X networks," *Internet Technology Letters*, vol. 7, no. 6, e489, 2024.
- [12] S. Sabeeh and K. Wesolowski, "Congestion Control in Autonomous Resource Selection of Cellular-V2X," *IEEE Access*, vol. 11, pp. 7450–7460, 2023.
- [13] Q. Fu, J. Liu, and J. Wang, "Per-Zone Resource Reuse for NR Sidelink Based Vulnerable Road User Protection," in *2023 International Wireless Communications and Mobile Computing (IWCMC)*, 2023, pp. 745–750.
- [14] A. Srivastava et al., "Enhanced Distributed Resource Selection and Power Control for High Frequency NR V2X Sidelink," *IEEE Access*, vol. 11, pp. 72 756–72 780, 2023.
- [15] H. Nguyen, M. Noor-A-Rahim, Y. L. Guan, and D. Pesch, "Performance Analysis of Cellular V2V Communications (LTE Mode-3 and 5G Mode-1) in the Presence of Big Vehicle Shadowing," in *2023 IEEE 34th Annual International Symposium on Personal, Indoor and Mobile Radio Communications (PIMRC)*, 2023, pp. 1–6.
- [16] Y. Yoon and H. Kim, "A Stochastic Reservation Scheme for Aperiodic Traffic in NR V2X Communication," in *2021 IEEE Wireless Communications and Networking Conference (WCNC)*, 2021, pp. 1–6.
- [17] L. Lusvarghi and M. L. Merani, "Machine Learning for Disseminating Cooperative Awareness Messages in Cellular V2V Communications," *IEEE Transactions on Vehicular Technology*, vol. 71, no. 7, pp. 7890–7903, 2022.
- [18] L. Cao, S. Roy, and H. Yin, "Resource Allocation in 5G Platoon Communication: Modeling, Analysis and Optimization," *IEEE Transactions on Vehicular Technology*, vol. 72, no. 4, pp. 5035–5048, 2023.
- [19] T. Eddine Toufik Djaidja, B. Briki, S. Mohammed Senouci, and Y. Ghamri-Doudane, "Adaptive Resource Reservation to Survive Against Adversarial Resource Selection Jamming Attacks in 5G NR-V2X Distributed Mode 2," in *ICC 2022 - IEEE International Conference on Communications*, 2022, pp. 3406–3411.
- [20] A. Chourasia, B. R. Tamma, and A. Antony Franklin, "Traffic-Aware Sensing-Based Semi-Persistent Scheduling for High Efficacy of C-V2X Networks," in *2021 IEEE 94th Vehicular Technology Conference (VTC2021-Fall)*, 2021, pp. 01–05.
- [21] L. Lusvarghi and M. L. Merani, "MoReV2X - A New Radio Vehicular Communication Module for ns-3," in *2021 IEEE 94th Vehicular Technology Conference (VTC2021-Fall)*, 2021, pp. 1–7.
- [22] A. Bazzi, C. Campolo, A. Molinaro, A. O. Berthet, B. M. Masini, and A. Zanella, "On Wireless Blind Spots in the C-V2X Sidelink," *IEEE Transactions on Vehicular Technology*, vol. 69, no. 8, pp. 9239–9243, 2020.
- [23] 3GPP, "Study on evaluation methodology of new Vehicle-to-Everything (V2X) use cases for LTE and NR;(Release 15)," 3GPP, TR 37.885 V15.3.0, Jun. 2019.
- [24] L. Lusvarghi, B. Coll-Perales, J. Gozalvez, and M. L. Merani, "Link Level Analysis of NR V2X Sidelink Communications," *IEEE Internet of Things Journal*, vol. 11, no. 17, pp. 28 385–28 397, 2024.
- [25] S. Nikooroo, J. Estrada-Jimenez, A. Machalek, J. Harri, T. Engel, and I. Turcanu, "Poster: Evaluating the Potential of Mode 2(b) Resource Allocation in NR V2X Sidelink," in *15th IEEE Vehicular Networking Conference (VNC 2024)*, Kobe, Japan: IEEE, May 2024.
- [26] 3GPP, "Enhancement of 3GPP support for V2X scenarios; Stage 1 (Release 18)," 3GPP, TS 22.186 V18.0.1, Mar. 2024.